

Modulatory effect of calmodulin-dependent kinase II (CaMKII) on sarcoplasmic reticulum Ca²⁺ handling and interval –force relations: a modelling study

Gentaro Iribe, Peter Kohl and Denis Noble

Phil. Trans. R. Soc. A 2006 **364**, 1107-1133
doi: 10.1098/rsta.2006.1758

References

[This article cites 47 articles, 21 of which can be accessed free](#)
<http://rsta.royalsocietypublishing.org/content/364/1842/1107.full.html#ref-list-1>

Rapid response

[Respond to this article](#)
<http://rsta.royalsocietypublishing.org/letters/submit/roypta;364/1842/1107>

Email alerting service

Receive free email alerts when new articles cite this article - sign up in the box at the top right-hand corner of the article or click [here](#)

To subscribe to *Phil. Trans. R. Soc. A* go to:
<http://rsta.royalsocietypublishing.org/subscriptions>

Modulatory effect of calmodulin-dependent kinase II (CaMKII) on sarcoplasmic reticulum Ca^{2+} handling and interval–force relations: a modelling study

BY GENTARO IRIBE*, PETER KOHL AND DENIS NOBLE

*Department of Physiology, Anatomy and Genetics, University of Oxford,
Sherrington Building, Parks Road, Oxford OX1 3PT, UK*

We hypothesize that slow inactivation of Ca^{2+} /calmodulin-dependent kinase II (CaMKII) and its modulatory effect on sarcoplasmic reticulum (SR) Ca^{2+} handling are important for various interval–force (I–F) relations, in particular for the beat interval dependency in transient alternans during the decay of post-extrasystolic potentiation. We have developed a mathematical model of a single cardiomyocyte to integrate various I–F relations, including alternans, by incorporating a conceptual CaMKII kinetics model into the SR Ca^{2+} handling model. Our model integrates I–F relations, such as the beat interval-dependent twitch force duration, restitution and potentiation, positive staircase phenomenon and alternans. We found that CaMKII affects more or less all I–F relations, and it is a key factor for integration of the various I–F relations in our model. Alternans arises, in the model, out of a steep relation between SR Ca^{2+} load and release, owing to SR load-dependent changes in the releasability of Ca^{2+} via the ryanodine receptor. Beat interval-dependent CaMKII activity, owing to its kinetic properties and amplifying effect on SR Ca^{2+} load dependency of Ca^{2+} release, replicated the beat interval dependency of alternans, as observed experimentally. Additionally, our model enabled reproduction of the effects of various interventions on alternans, such as the slowing or accelerating of Ca^{2+} release and/or uptake. We conclude that a slow time-dependent factor, represented in the model by CaMKII, is important for the integration of I–F relations, including alternans, and that our model offers a useful tool for further analysis of the roles of integrative Ca^{2+} handling in myocardial I–F relations.

Keywords: mechanical alternans; calcium/calmodulin-dependent kinase; sarcoplasmic reticulum

1. Introduction

The mechanical characteristics of extrasystolic (ES) beat and post-extrasystolic potentiation (PESP) are strongly linked to beat intervals: the shorter the ES interval (ESI), the smaller the ES beat, and the larger the subsequent PESP. This relation has been well described in the context of restitution and potentiation, conventionally presented by interval–force (I–F) relations (Wier & Yue 1986).

* Author for correspondence (gentaro.iribe@physiol.ox.ac.uk).

One contribution of 13 to a Theme Issue ‘Biomathematical modelling I’.

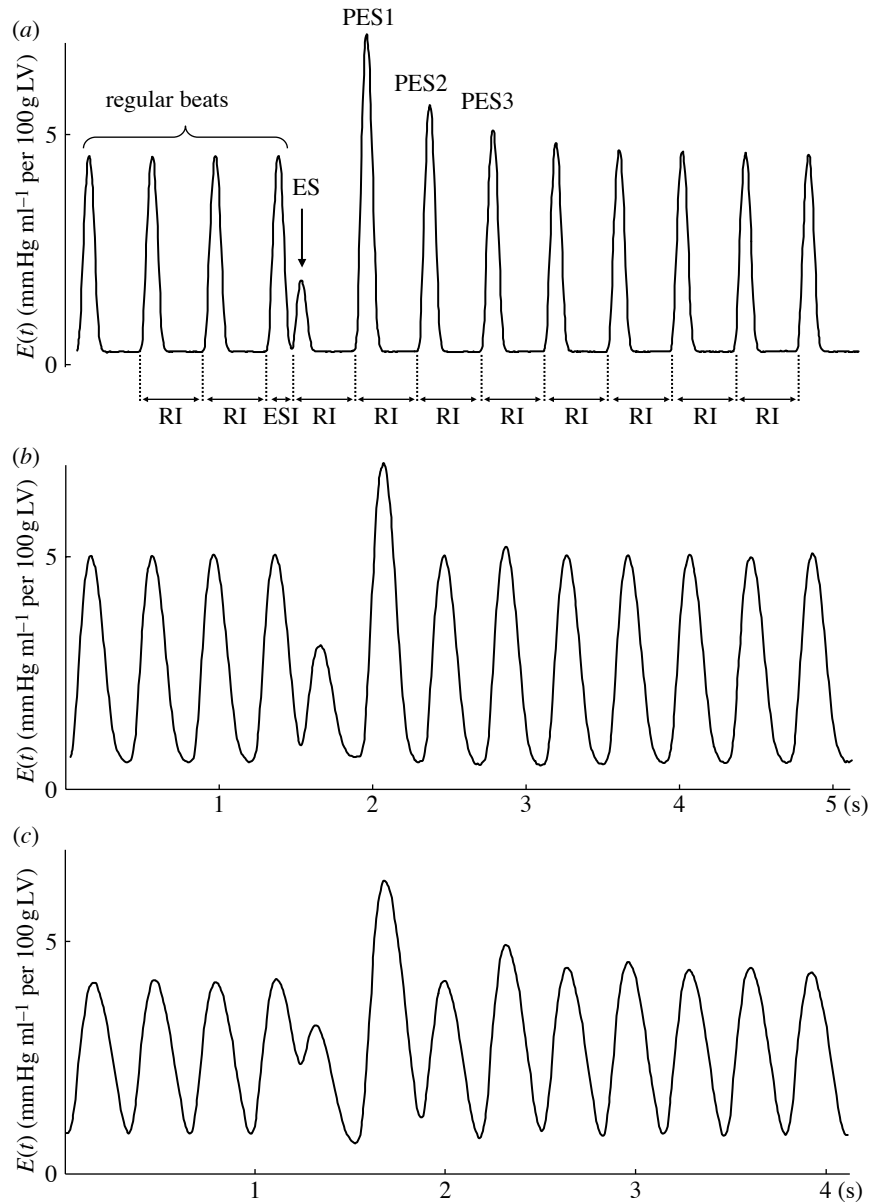


Figure 1. Frequency dependence of transient alternans during the decay of post-extrasystolic (PES) potentiation (PESP) in excised cross-circulated canine heart (G. Iribe, J. Shimizu & H. Suga 2002, unpublished data). (a) A monotonic PESP decay was observed after 1 min of pacing at a regular interval (RI) of 0.75 s, followed by an extrasystolic interval (ESI) of 0.3 s. (b) Slight transient alternans was seen during the decay of PESP after pacing at RI=0.4 s and ESI=0.3 s. (c) More pronounced transient alternans of PESP decay at RI=0.33 s and ESI=0.25 s.

The dynamics of PESP decay is also affected by the beat interval (Shimizu *et al.* 2000). Rapid pacing, for example, may lead to pronounced mechanical alternans of the decay pattern, with a positive correlation between stimulation rates and alternans amplitude (figure 1; Kihara & Morgan

1991; Laurita *et al.* 2003). Owing to this beat interval dependency, transient alternans during the decay of PESP may be interpreted as an integral constituent of I–F relations. It is this ‘broad conceptual approach’ that underlies the concept of I–F relations in this paper (i.e. any force change induced by beat interval variations).

Although transient mechanical alternans may be brought about by either haemodynamic or cellular contractile mechanisms (Lab & Seed 1993; Iribe *et al.* 2004), recent studies suggest transient alternation of the contractile state of cardiomyocytes as a primary mechanism, based in particular on periodic alterations in intracellular Ca^{2+} cycling, rather than membrane ionic currents (Diaz *et al.* 2004; Pruvot *et al.* 2004). Although the detailed mechanisms that give rise to mechanical alternans are still not clear, time-dependent changes in sarcoplasmic reticulum (SR) Ca^{2+} handling may hold a key to understanding this phenomenon (Diaz *et al.* 2004).

It has been revealed that the Ca^{2+} /calmodulin-dependent kinase II (CaMKII) plays an important role in regulating Ca^{2+} handling by phosphorylating several Ca^{2+} transporting proteins, such as ryanodine receptors (RyR) (Witcher *et al.* 1991) and phospholamban (Davis *et al.* 1983). CaMKII is activated upon increased cytosolic Ca^{2+} concentration ($[\text{Ca}^{2+}]_i$) as a result of formation of Ca^{2+} -calmodulin (Ca^{2+} -CaM) complexes. Once CaMKII binds Ca^{2+} -CaM, the regulatory domain of the enzyme (Thr-286) is auto-phosphorylated. Auto-phosphorylation increases the affinity of CaM and CaMKII. This effect traps CaM on CaMKII. Therefore, the enzyme remains active for several seconds even when $[\text{Ca}^{2+}]_i$ decreases to resting level (Meyer *et al.* 1992; Maier & Bers 2002). These properties provide CaMKII with relatively slow inactivation kinetics, of the order of several seconds (Braun & Schulman 1995). The CaMKII activity levels that result from the increase in $[\text{Ca}^{2+}]_i$ during one beat may affect Ca^{2+} handling, and mechanical output, during the subsequent beats. The extent to which this occurs is determined by the beat interval, which renders the slow inactivation of CaMKII as potentially important for I–F relations.

In the present study, we investigate the hypothesis that the beat interval dependency of transient alternans during the decay of PESP may be explained by CaMKII-dependent changes in SR Ca^{2+} handling. To test the viability of this hypothesis, we developed a mathematical model of SR Ca^{2+} handling that takes into account CaMKII dynamics. We incorporated this SR model into the *OxSoft* ‘electric’ cardiomyocyte model (i.e. the description of membrane currents, transporters and compartments) of Noble *et al.* (1991), combined with the ‘mechanics’ model of Rice *et al.* (1999). We also aimed to make the model as complex as necessary and as simple as possible, to help identification of causally linked events, and for computing efficiency. Using this model, we investigate the Ca^{2+} dynamics during various protocols and I–F relations, and assess the involvement of CaMKII in determining the beat interval dependency of transient alternans during the decay of PESP. Our model shows that CaMKII involvement in Ca^{2+} handling not only successfully reproduces the beat interval dependency of alternans, but integrates alternans and various other I–F relations at the whole cell level.

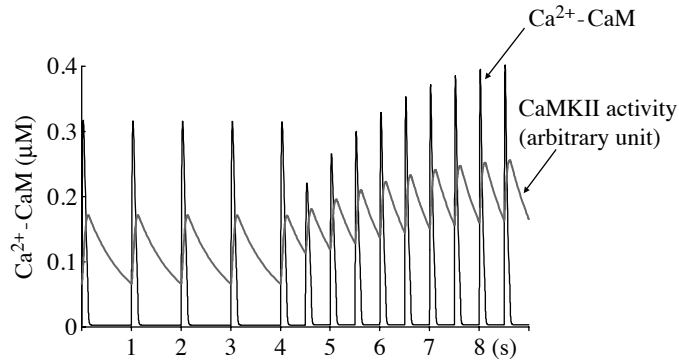


Figure 2. Simulated effect of 'slow inactivation' of the conceptual Ca^{2+} /calmodulin-dependent kinase II (CaMKII) activity term on Ca^{2+} -calmodulin (Ca^{2+} -CaM) activity during a sudden increase in pacing rate (from 1 to 2 Hz).

2. Method

(a) Model description

(i) CaMKII kinetics model

Since the detail of dynamic beat-to-beat changes in CaMKII activity is still not fully resolved, we added a conceptual CaMKII kinetics term to describe its involvement in I-F relations. To mimic known properties of CaMKII kinetics, the enzyme activity of the Ca^{2+} -CaM-CaMKII complex can be expressed as a function of Ca^{2+} -CaM, with a rapid binding rate and slow dissociating rate. We calculate an enzyme activity factor (arbitrary units) using equation (A 49) (see appendix A for a complete listing of equations underlying the present model; all further reference to equation numbers relates to this appendix). Figure 2 illustrates how Ca^{2+} -CaM and Ca^{2+} -CaM-CaMKII change in our model when the pacing rate is altered from 1 to 2 Hz. The enzyme activity term dampens changes in Ca^{2+} -CaM. This 'slow inactivation' results in a higher CaMKII activity during shorter beat interval, compared with regular ones.

(ii) SR Ca^{2+} release model

The three-state model of the RyR used in this model is based on the formulations by Hilgemann & Noble (1987). It describes inactivation and recovery processes of RyR via precursor (F_1 in equation (A 42)), activator (F_2 in equation (A 43)) and product fraction (F_3 in equation (A 44)). RyR activation and inactivation rates are based on the Kyoto model (Matsuoka *et al.* 2003). The Ca^{2+} -induced activation rate (k_1 in equation (A 45)) is defined as a function of $[\text{Ca}^{2+}]_i$ and L-type Ca^{2+} channel current (I_{CaL}). The inactivation rate (k_2 in equation (A 46)) is defined as a function of the SR Ca^{2+} concentration $[\text{Ca}^{2+}]_{\text{SR}}$. The rate of recovery of RyR (k_3 in equation (A 47)) is a function of $[\text{Ca}^{2+}]_{\text{SR}}$ (to express the SR load dependency of the open probability), and the modulating effect of CaMKII on Ca^{2+} release (Li *et al.* 1997) is included in it. Additionally,

we incorporate an SR load dependency of Ca^{2+} conduction through RyR (Gyorke & Gyorke 1998; Ching *et al.* 2000) into our model (A 39).

(iii) *SR Ca^{2+} uptake model*

CaMKII regulates phosphorylation of phospholamban, which enhances SR Ca^{2+} -ATPase (SERCA) activity and SR Ca^{2+} uptake. CaMKII involvement in SR Ca^{2+} uptake contributes to the interval dependence of twitch duration (Schouten 1990; Bassani *et al.* 1995), and it may be expected to affect I–F relations as well. To describe this CaMKII involvement, we use the SERCA model of Shannon *et al.* (2000) and added a CaMKII dependency in the forward (uptake) flux of SERCA (A 51).

(iv) *SR and cytosolic compartments*

Many of the recent cardiac cell models assume two compartments for the SR: one Ca^{2+} uptake site, and one release site, with considerable delay in Ca^{2+} transfer from uptake to release site. However, some recent data suggest that Ca^{2+} diffusion should be quick enough to cause very little difference in Ca^{2+} concentration between sites (Shannon *et al.* 2003). Therefore, the present model uses a single compartment for the SR (for simplicity and lack of better experimental data). Furthermore, many recent models assume the dyadic space as a uniform site for Ca^{2+} entry into the cytosol via L-type Ca^{2+} channels and RyR (Nordin 1993; Rice *et al.* 2000). Since modelling of the dyadic space is not essential for studying beat-to-beat integrative Ca^{2+} dynamics in I–F relations, we use only one compartment for the cytosolic space to calculate $[\text{Ca}^{2+}]_i$ (A 58).

(v) *Contraction model*

To evaluate I–F relations taking into account Ca^{2+} dynamics, the force computation model describes interactions between force and Ca^{2+} in relative detail. We use the model of contraction and cooperativity mechanisms of Ca^{2+} , troponin, tropomyosin and crossbridge formation by Rice *et al.* (1999). Not only a feed-forward pathway from changes in $[\text{Ca}^{2+}]_i$ to force production, but also a feedback pathway from developed force to Ca^{2+} handling and troponin binding (A 55) are included.

(vi) *Other components*

As mentioned earlier, many recent models assume a dyadic space (Nordin 1993; Rice *et al.* 2000), thus L-type Ca^{2+} channel formulations in such models are optimized to account for the presence of such a space. Our present model does not separate the dyadic space; therefore, for membrane currents, we incorporate a previously published single cardiac cell model, which does not have a dyadic space, by Noble *et al.* (1991) (as opposed to Noble *et al.* (1998), for instance). Appendix A gives the full set of equations. The CELLML version of the model will be available on http://www.cellml.org/models/iribe_kohl_noble_2006_version01.

(b) Experimental protocols

The model was validated against published experimental information on Ca^{2+} dynamics in relation to I–F relations, including the interval dependence of twitch duration, restitution and potentiation, and the staircase phenomenon. On this basis, we investigate the behaviour of alternant decay of PESP, and suggest experimentally testable hypotheses regarding the mechanisms that may underlie this phenomenon. The detail of each pacing protocol is explained in §3.

The simulations were run on MATLAB, using ode15s (Runge–Kutta) as the solver for integrating the ordinary differential equations.

3. Results*(a) Interval dependence of twitch duration*

It has previously been reported that twitch duration decreases when the preceding beat interval is shortened (Schouten 1990; Bassani *et al.* 1995). The mechanism proposed here is as follows: after a short interval, SERCA is still activated because of the slow inactivation of CaMKII (figure 2); therefore, SR Ca^{2+} uptake is enhanced, leading to more rapid relaxation.

Figure 3*a* illustrates the approach to assessing the interval dependence of twitch duration in the model. After pacing the model for 20 s at 1 Hz (to obtain a sufficiently steady control state), an ES beat is introduced at an ESI of either 0.5 or 2 s (figure 3*a*). Time from stimulus to peak force (PFT) and twitch duration at relaxation to 50% of the peak force (TD_{50}) are compared for the ES beats (figure 3*b*). PFT and TD_{50} are reduced at short ESI (0.069 and 0.138 s, respectively) and increased at long ESI (0.099 and 0.167 s, respectively), compared to control activity (0.084 and 0.154 s, respectively), as seen in experiments (Schouten 1990; Bassani *et al.* 1995). Figure 3*c,d* shows superimposed SR Ca^{2+} uptake flux curves and CaMKII activities for both ES beats (ESI = 0.5 and 2 s). The uptake flux is larger at the shorter ESI, because of elevated CaMKII activity (peak flux of 0.181 and 0.158 mM s^{-1} in ESI at 0.5 and 2 s, respectively). These simulations reproduce, in principle, the phenomena and mechanism highlighted in the experiments of Schouten and Bassani (Schouten 1990; Bassani *et al.* 1995).

(b) Mechanical restitution and potentiation

Figure 4 shows the results of experiments to characterize mechanical restitution and potentiation in our model. After conditioning cells to a steady state by fixed rate pacing (0.5 Hz), ES beats are introduced at variable ESI (from 0.4 to 2 s), followed by a PES beat at a fixed interval of 2 s (figure 4*a*). As shown in figure 4*a*, ES amplitude increases with ESI, while PESP shows the opposite trend. This is consistent with experimental observations by Wier & Yue (1986).

The key mechanism underlying restitution of ES beat amplitude is recovery of RyR releasability (defined in the model as the product of RyR flux factor and release fraction of RyR, $K_{\text{rel}} \times F_{\text{rel}}$; see appendix A for more detail, and figure 4*b*), while PESP dynamics are mainly linked to SR Ca^{2+} content (figure 4*c*), as previously modelled by Rice *et al.* (2000).

Our model further reveals a possible contribution of CaMKII to these phenomena. The shorter the ESI, the greater the CaMKII activity (figure 4*d*).

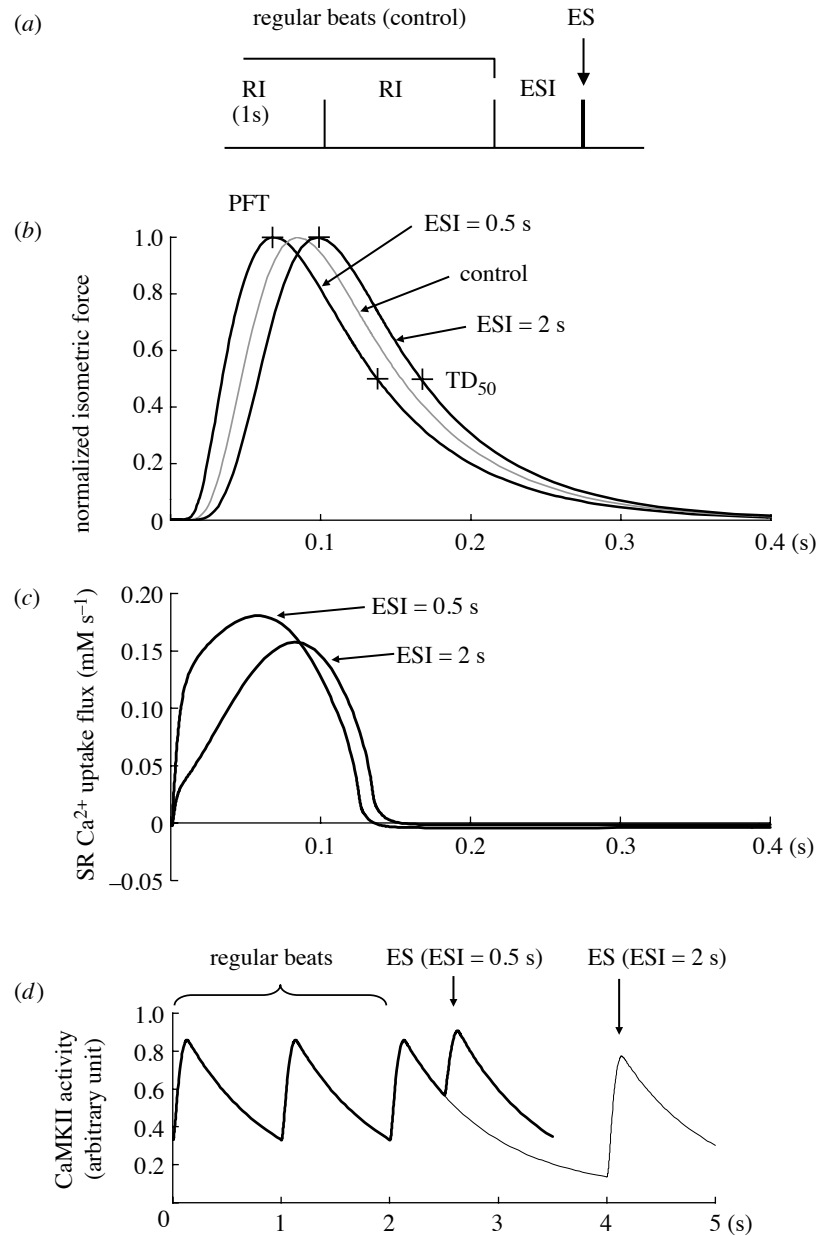


Figure 3. Interval dependence of twitch amplitude and duration. (a) Pacing protocol. After obtaining a steady state, an extrasystole (ES) is introduced, using an ESI of either 0.5 or 2 s. (b) Superimposed normalized force curves of ES beats at 0.5 and 2 s ESI (control regular beat is shown in grey). Time from stimulus to peak force (PFT) and twitch duration at 50% relaxation (TD₅₀) are shorter at an ESI of 0.5 s than at 2 s. (c) Superimposed SR Ca²⁺ uptake flux curves of ES beats after 0.5 and 2 s ESI. The shorter ESI is associated with a larger Ca²⁺ uptake. (d) Superimposed CaMKII activity curves for both ESI. In contrast to an ESI of 2 s, CaMKII is re-activated before complete inactivation with an ESI of 0.5 s.

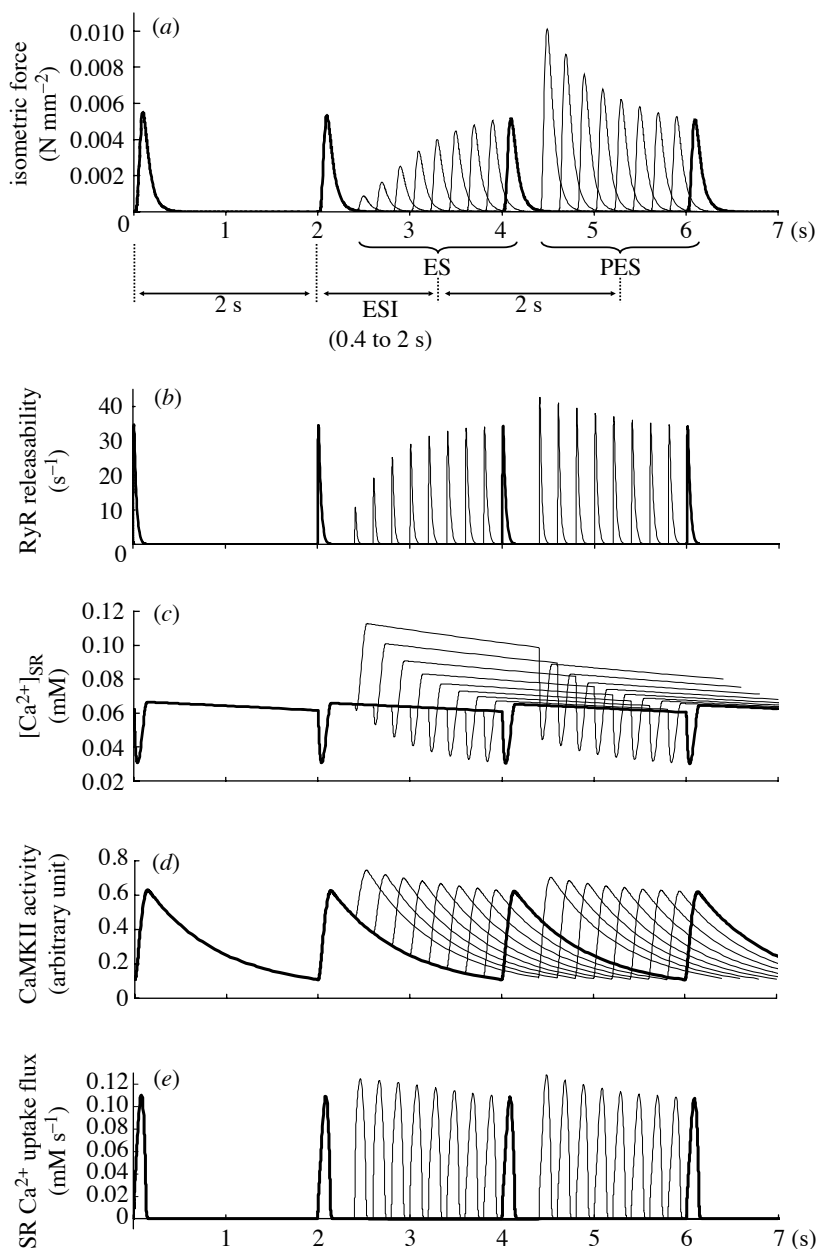


Figure 4. Restitution and potentiation properties. (a) Pacing protocol. After regular pacing at 0.5 Hz, an ES beat is introduced after variable ESI from 0.4 to 2 s. Subsequent PES stimuli were applied after a constant 2 s interval. (b) RyR releasability. (c) SR Ca²⁺ content. (d) CaMKII activity. (e) SR Ca²⁺ uptake flux.

Therefore, although Ca²⁺ release from RyR is small after a short ESI, SR Ca²⁺ uptake is increased (compared to control; figure 4e). This biases Ca²⁺ handling towards sequestration, so that less Ca²⁺ reaches troponin C, thereby reducing force generation. CaMKII also affects PES. The increased SR load after a

shorter ESI (main mechanism for PESP) is not only caused by preservation of Ca^{2+} in the SR (reduced release via non-recovered RyR), but also by an enhanced Ca^{2+} uptake into the SR via CaMKII effects. Additionally, RyR releasability during the PES period is also enhanced because of its SR load dependency and the amplifying effect of CaMKII on this load dependency (figure 4*b,d*). These effects lead to more prominent potentiation during the PES period compared to the model without CaMKII involvement (Nordin 1993; Rice *et al.* 2000).

(*c*) *Positive staircase phenomenon*

Increasing stimulation frequency gives rise to a positive inotropic effect via increasing SR Ca^{2+} content and release in many species (Kurihara & Sakai 1985; Maier *et al.* 2000). This phenomenon can be reproduced by the model. Figure 5 illustrates the effects of changing stimulation rate from 1 to 2 Hz, and then back to 1 Hz. The initial drop in twitch force amplitude at the onset of 2 Hz stimulation (figure 5*a*) reflects the reduced fraction of recovered RyR channels at the faster pacing rate (figure 5*d*). Thereafter, SR Ca^{2+} content is gradually raised by the enhanced SR Ca^{2+} uptake, caused in the model by increased CaMKII activity (figure 5*b,c*). SR Ca^{2+} release is additionally enhanced via SR Ca^{2+} load dependency of Ca^{2+} releasability. This is also related to the increased CaMKII activity (figure 5*c,d*).

Conversely, reduction of pacing rate from 2 to 1 Hz causes a transient increase in twitch force via additional recovery of RyR channels. Thereafter, SR Ca^{2+} gradually returns to control levels, as the reduced CaMKII activity decreases SR Ca^{2+} uptake and Ca^{2+} releasability.

(*d*) *Mechanisms of transient alternans of PESP decay*

To examine Ca^{2+} handling during the transient alternans of the PESP decay in our model, we use the pacing protocol illustrated in figure 6*a*. After a control pacing cycle at a steady state regular interval (RI) of between 0.4 and 0.75 s, ES beats are introduced at an ESI that is shorter than RI (see figure 6 legend for detail). After one ES beat, pacing rate is restored to record PESP and its decay dynamics (see figure 1 for experimental and figure 6 for modelling findings).

Depending on the background pacing rate, alternans of the PESP decay pattern has been observed in experiments of mammalian myocardium, where alternans is most pronounced at faster pacing rates (Kihara & Morgan 1991; Laurita *et al.* 2003). The model reproduces this beat interval dependency of alternans in PESP decay (compare figures 1 and 6*a*). At RI of 0.75 s, PESP decays monotonically, both in experiment and model. Increasing RI (to 0.4 s in experiments and to 0.5 s in the model) gives rise to minor oscillations in PESP amplitudes. Clear mechanical alternans can be observed at even shorter RI (0.33 s in experiments, 0.4 s in the model).

Diaz *et al.* (2004) showed that mechanical alternans is caused by beat-to-beat alternation in $[\text{Ca}^{2+}]_i$, which in turn is mainly due to the alternation in SR Ca^{2+} content. In particular, the steepness of the relation between SR Ca^{2+} content and Ca^{2+} release is critical in the induction of mechanical alternans. Our results show that mechanical alternans during PESP decay is linked to SR Ca^{2+} content fluctuations (figure 6*a*, right-hand side).

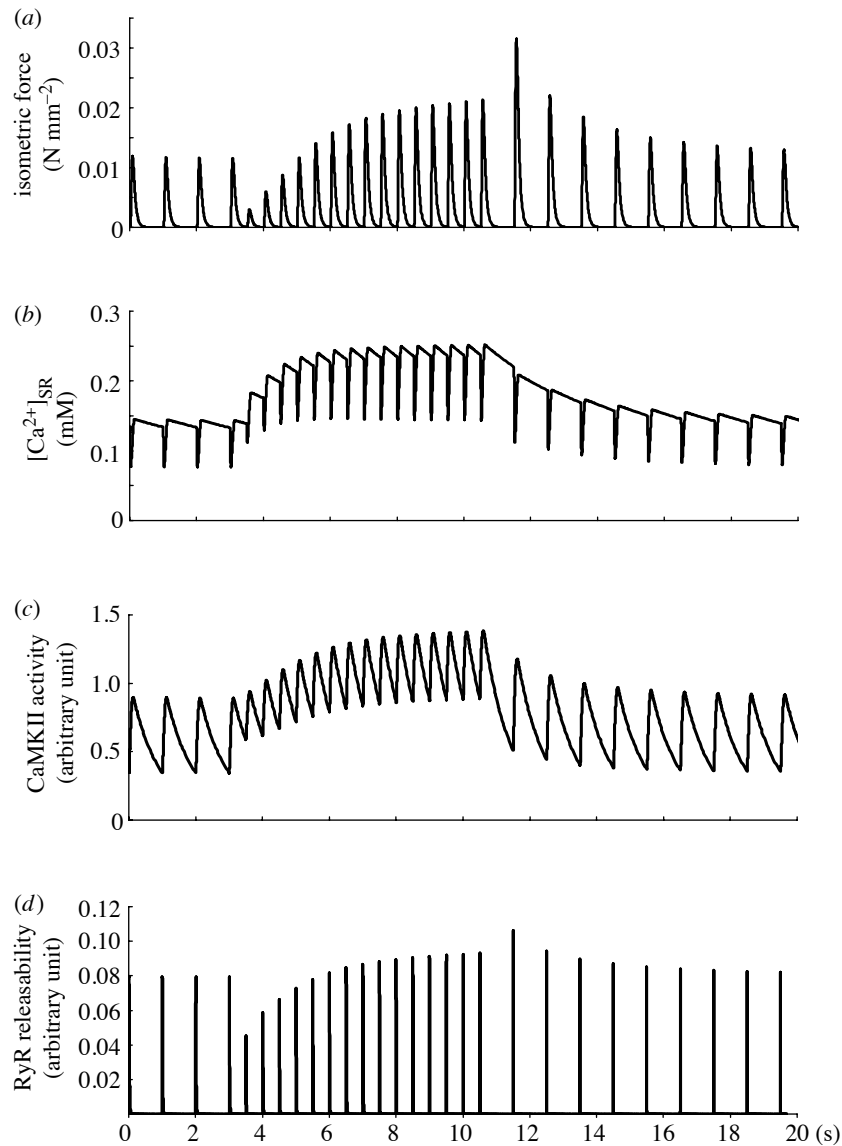


Figure 5. Positive staircase phenomenon. Stimulation frequency is changed from 1 to 2 Hz, and back. (a) Isometric force. (b) SR Ca^{2+} content. (c) CaMKII activity. (d) RyR Ca^{2+} releasability.

Figure 6*b* summarizes the relation between SR Ca^{2+} load and Ca^{2+} release of several PES beats (same cases as in figure 6*a*). SR Ca^{2+} load is equal to the value of $[\text{Ca}^{2+}]_{\text{SR}}$ prior to the stimulation, while SR Ca^{2+} release is the difference between SR Ca^{2+} load and the smallest $[\text{Ca}^{2+}]_{\text{SR}}$ reached during any given beat. At an RI of 0.75 s, the slope of this relation is shallow, which means that SR Ca^{2+} content decreases gradually, which results in a monotonic decay of PESP. At RI of 0.4 s, the slope of the relation is steeper, supporting large SR Ca^{2+} releases during the first PES beat (because of the high SR load). This large release reduces SR Ca^{2+} load; therefore, the next SR release (and resultant PES

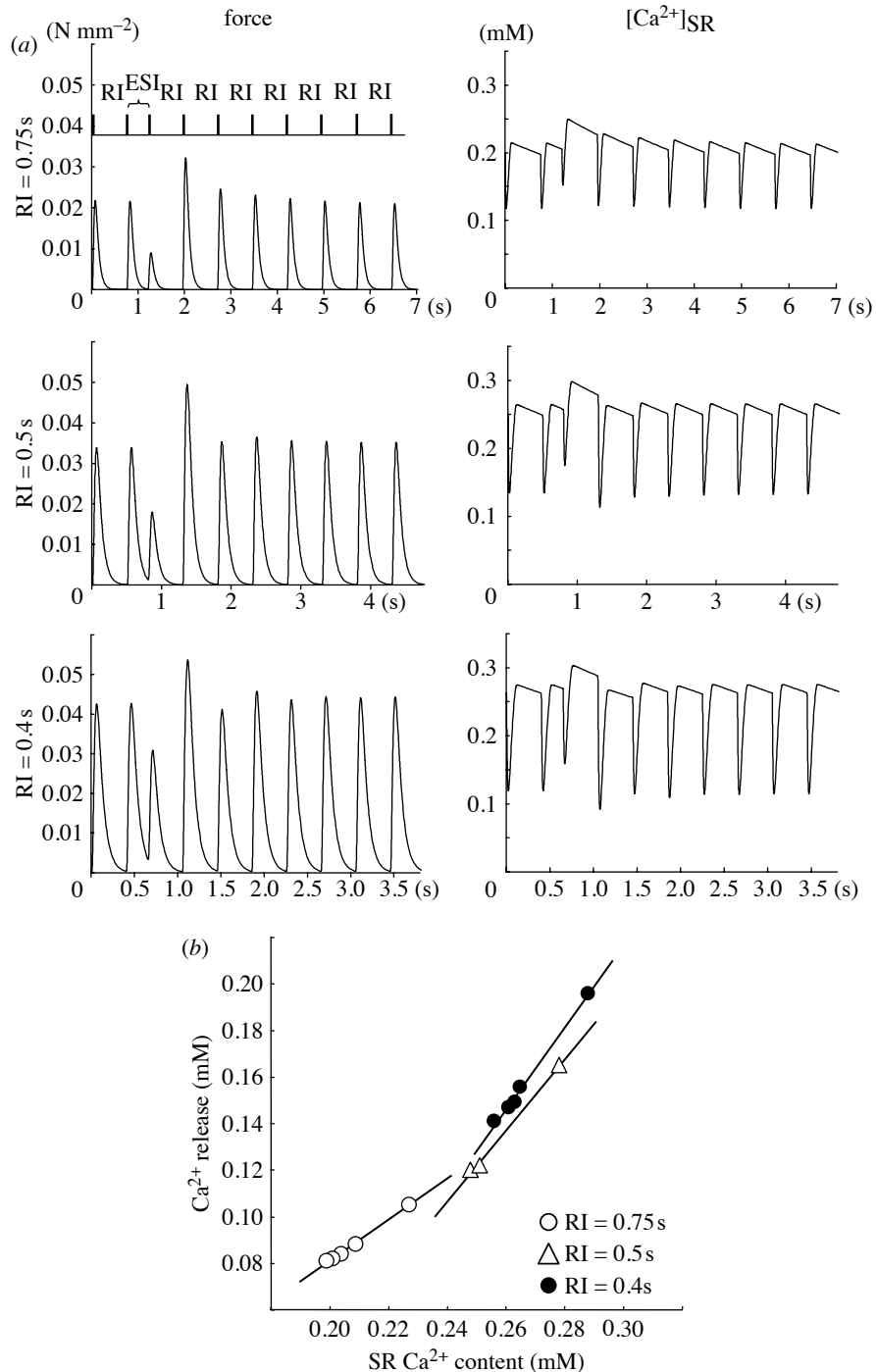


Figure 6. Frequency dependency of transient alternans during PESP decay. (a) Isometric force (left) and SR Ca^{2+} content (right) at RI of 0.75, 0.5 and 0.4 s (from top to bottom); with ESI of 0.45, 0.3 and 0.25 s, respectively. (b) Relation between SR Ca^{2+} load and Ca^{2+} release of several PESP beats (same data as in (a)).

beat) are small. This small SR Ca^{2+} release increases SR Ca^{2+} content in relative terms (but not to the same level as observed before the first beat), giving rise to transient alternans of the PESP decay pattern, as seen experimentally (Diaz *et al.* 2004). Accordingly, the ‘beat interval dependency of alternans’ could also be referred to as a ‘beat interval-dependent change in SR Ca^{2+} load dependency of Ca^{2+} release’. In the present model, this feature is brought about by an enhancing effect of CaMKII on the SR Ca^{2+} load-dependent RyR recovery rate (k_3 ; (A 47)). More rapid stimulation results in higher CaMKII activity, which steepens the relations between SR Ca^{2+} content and Ca^{2+} release, and causes increasingly pronounced mechanical alternans of the PESP decay.

In addition to its beat interval dependency, mechanical alternans has also been observed upon slowing of either RyR or SERCA (Diaz *et al.* 2002; Kameyama *et al.* 2003; Kockskamper *et al.* 2005). Figure 7*a* shows the effects of slowing or accelerating the transition between the three functional states of RyR, presented in the model, on alternans during PESP decay. This is based on the ‘intermediate’ scenario in figure 6*a* (RI=0.5 s), for comparison. Slowing all transition rates by 20% significantly enhanced alternans, while an equally pronounced acceleration eliminates alternans. This result is consistent with previous experimental findings (Diaz *et al.* 2002). Figure 7*b* shows superimposed traces of Ca^{2+} releasability during both slowed and accelerated RyR dynamics in the first and second PES beat (note the fluctuation in amplitude of Ca^{2+} releasability when RyR function is slowed, also present when accelerated, though to a lesser extent). During the first PES beat, slowed RyR give rise to a slightly smaller peak releasability compared to the accelerated RyR. However, slowed RyR stay open for longer, so that overall more Ca^{2+} is released. This causes a more pronounced Ca^{2+} depletion of the SR and contributes to reduced Ca^{2+} release during the subsequent beat. During the second PES beat, slow RyR are still open for longer, but peak releasability is considerably smaller than in the presence of accelerated RyR (because of the SR Ca^{2+} load dependency of RyR releasability), which also contributes to the overall reduction in SR Ca^{2+} release during the second beat with slowed RyR. This behaviour makes the slope of the relationship between SR Ca^{2+} load and Ca^{2+} release steeper, as summarized in figure 7*c*, and leads to more pronounced alternans in the presence of slowed RyR.

Thus, although both rapid pacing and slowed RyR dynamics introduce/enhance alternans by increasing the steepness of the relationship between SR Ca^{2+} load and Ca^{2+} release, the primary mechanisms underlying these effects are different. In the case of rapid pacing, the steep relation is induced by increased CaMKII activity; while in the case of slowed RyR it is caused by prolonged RyR opening.

To investigate the experimentally observed effects of SR Ca^{2+} uptake rates on alternans, we slowed or accelerated the Ca^{2+} uptake rate parameter (V_{maxf}). Figure 8*a* illustrates the enhancement of alternans in the PESP decay pattern (compared to the ‘intermediate’ control scenario illustrated in figure 6*a*; RI=0.5 s), that is caused by a 20% slowing of Ca^{2+} uptake rate. A matching increase in SERCA activity eliminates alternans. This result is consistent with previous experimental findings (Kameyama *et al.* 2003; Kockskamper *et al.* 2005).

In the model, slowed SERCA activity reduces Ca^{2+} sequestration into the SR during RyR release, thereby causing an increase in the first PES beat compared

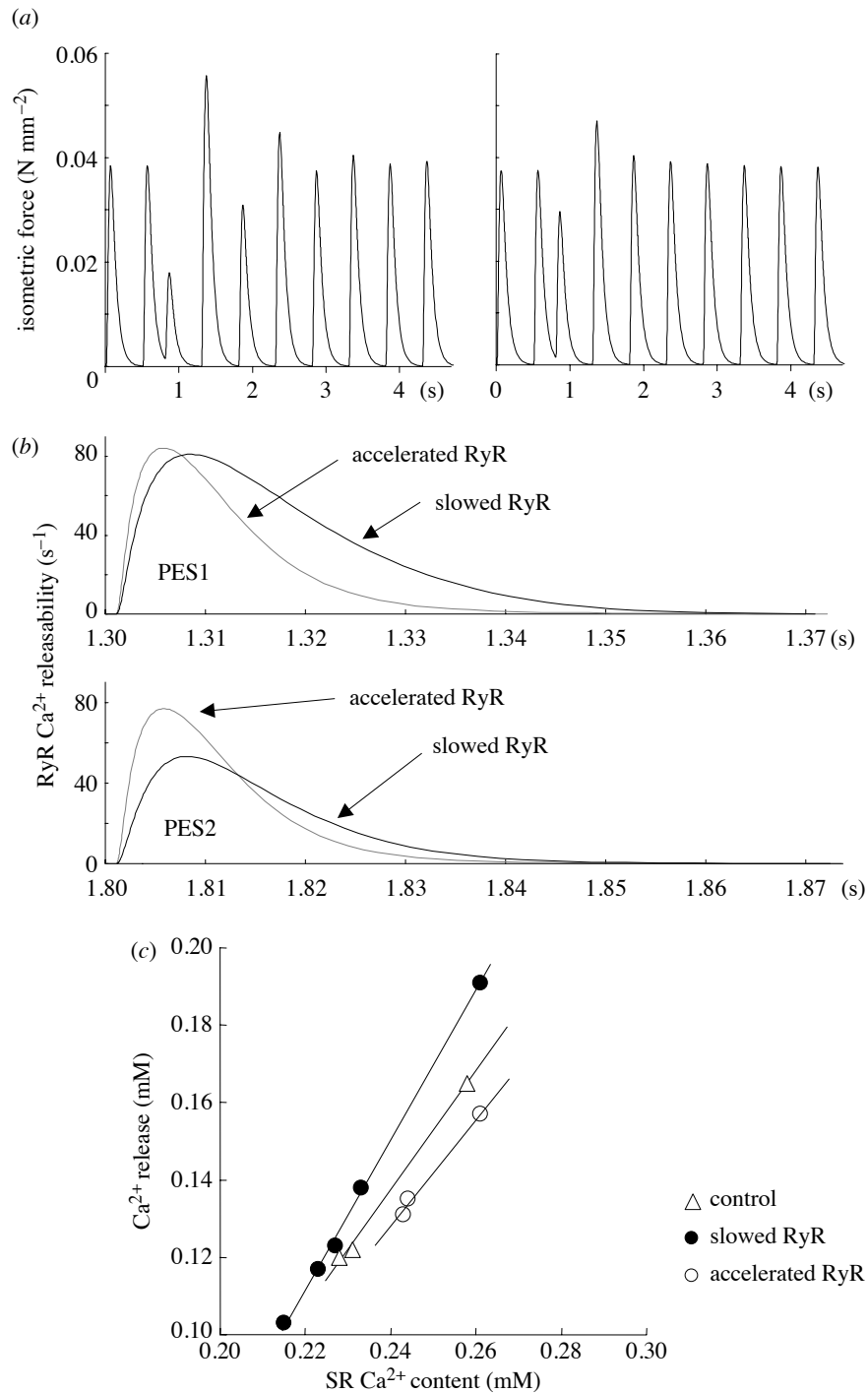


Figure 7. Effect of slowing or accelerating the state transition rate of RyR on transient alternans of PESP decay. (a) Isometric force with slowed (left) and accelerated (right) RyR. (b) Superimposed RyR Ca²⁺ releasability curves of the first (PES1) and second (PES2) PES beats. (c) Relation between SR Ca²⁺ load and Ca²⁺ release (control data from RI=0.5 s in figure 6b).

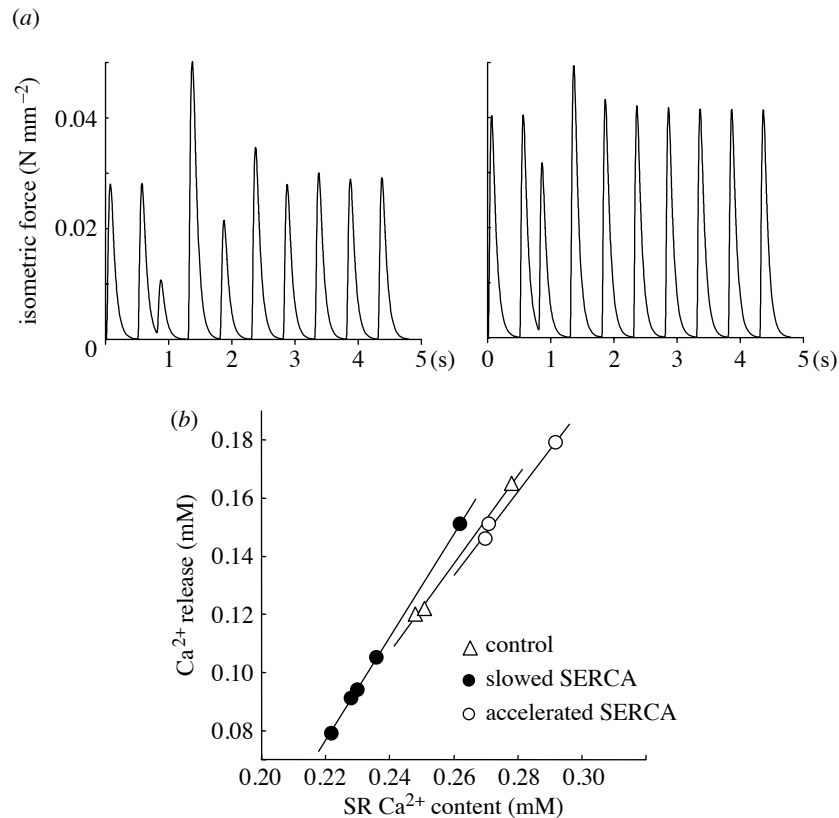


Figure 8. Effect of slowing or accelerating SR Ca²⁺ uptake on transient alternans of PESP decay. (a) Isometric force with slowed (left) and accelerated (right) SERCA. (b) Relation between SR Ca²⁺ load and Ca²⁺ release (control data from RI=0.5 s in figure 6b).

to control (which makes the slope of the relation between SR Ca²⁺ content and Ca²⁺ release steep). The reduced SERCA activity shifts the balance of Ca²⁺ handling from preservation in the SR to extrusion through the sarcolemma, which reduces the second PES beat.

With accelerated SERCA activity, Ca²⁺ that is being released via RyR is partially sequestered back into the SR, even while RyR release is still ongoing. This reduces the overall amount of SR Ca²⁺ release during the first PES beat and the amplitude of PESP. In addition, the enhanced SERCA activity increases Ca²⁺ re-uptake into the SR, raising Ca²⁺ content for the second beat. From there on, PES beat amplitude decays monotonically.

Figure 8b summarizes the relationship between SR Ca²⁺ content and Ca²⁺ release with slowed and accelerated Ca²⁺ uptake dynamics. Although the properties of RyR in both cases are identical, the slope of the relationship is somewhat shallower in the case with accelerated uptake.

CaMKII effects on SR Ca²⁺ uptake may play a role in the genesis of alternans. Therefore, we tested transient alternans of the PESP decay in the presence and absence of CaMKII fluctuations, as shown in figure 9. Using the ‘intermediate’ case of figure 6a as a control (RI=0.5 s; figure 9, left-hand side), we set CaMKII

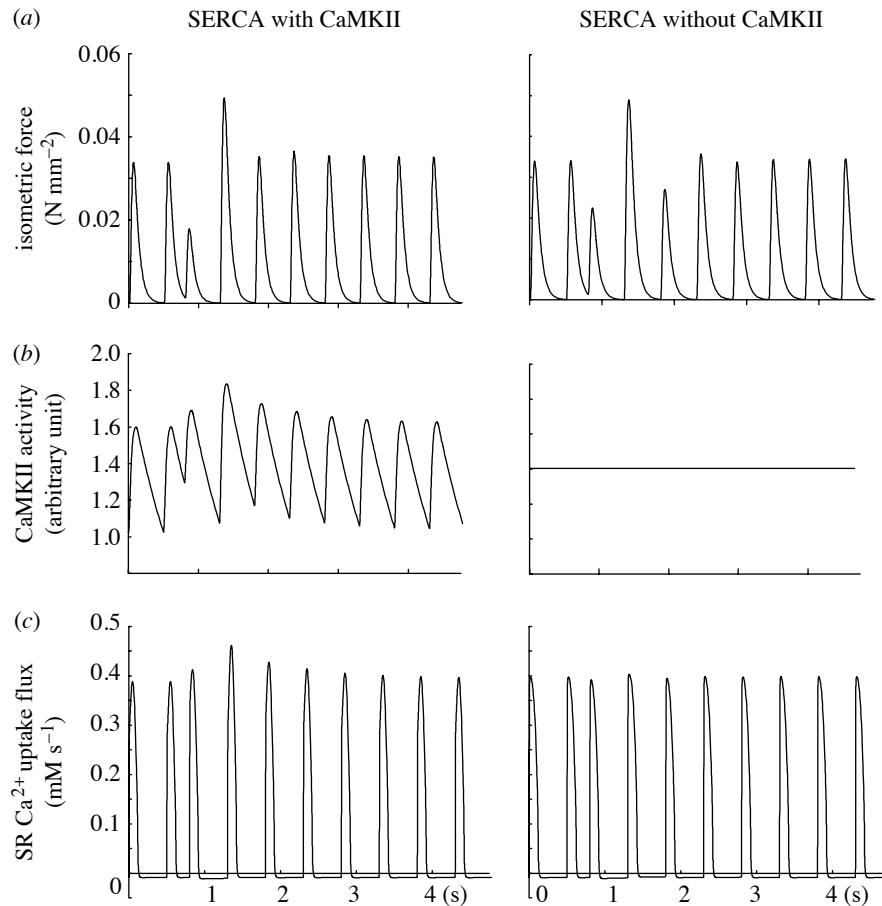


Figure 9. Effect of CaMKII involvement in SR Ca^{2+} uptake on transient alternans during PESP decay. (a) Isometric force with (left) and without (right) CaMKII involvement in modulating SR Ca^{2+} uptake. (b) CaMKII activity on SERCA. In the case without CaMKII involvement, the activity value was set to a fixed value at intermediate levels of the dynamic setting (right). (c) SR Ca^{2+} uptake flux with (left) and without (right) CaMKII involvement.

activity factor (F_{CaMK}) in the Ca^{2+} uptake formula (A 51) to its average value in control conditions (figure 9, right-hand side). As shown in figure 9a, CaMKII modulation of Ca^{2+} uptake reduces alternans. Figure 9b,c shows CaMKII activity and SR Ca^{2+} uptake flux, respectively. CaMKII activity in the PES period is higher than that in steady state. Therefore, Ca^{2+} uptake is higher during the PES period in the presence of functional CaMKII. Especially, after the first PES beat, enhanced Ca^{2+} uptake prevents depletion of SR Ca^{2+} content at the next beat. As a result, the second PES beat becomes larger than it would have been without CaMKII involvement, thereby reducing alternans.

This result may be seen as somewhat counter-intuitive, as one might have expected that an increased CaMKII activity at the beginning of the second PES beat would sequester more Ca^{2+} and reduce the amplitude of the second PES beat over and above the level seen without CaMKII involvement. However, the

model predicts that the effect of CaMKII on preserving SR Ca^{2+} content (enhancing uptake) after the first PES beat dominates over the reducing effect on the second PES beat.

4. Discussion

Several myocardial Ca^{2+} handling models have been proposed to describe and study alternans (Adler *et al.* 1985; Snyder *et al.* 2000; Tameyasu 2002; Shiferaw *et al.* 2003). Each of them features Ca^{2+} handling in different detail. However, a common and apparently fundamental mechanism underlying alternans is a steep relation between SR Ca^{2+} load and Ca^{2+} release, which is also supported by experimental evidence (Diaz *et al.* 2002).

Some of the existing models allow one to replicate the beat interval dependency of alternans. For example, Snyder *et al.* (2000) describe this phenomenon as instability in the bi-directional feedback system between RyR and calsequestrin during rapid pacing, while Shiferaw *et al.* (2003) explain it as a result of variable Ca^{2+} -induced inactivation of L-type Ca^{2+} channels, due to increasing diastolic $[\text{Ca}^{2+}]_i$ during rapid pacing. Our model proposes an alternative concept, where CaMKII is a major contributor to the beat interval dependency of alternans. This is in keeping with data from Li *et al.* (1997), who reported that CaMKII increased the amount of SR Ca^{2+} release for a given SR Ca^{2+} content and I_{CaL} trigger in intact voltage clamped ventricular myocytes. They showed a shallower relationship between SR Ca^{2+} load and twitch $[\text{Ca}^{2+}]_i$ under CaMKII inhibition than in control. This suggests that CaMKII modulation of the relation between SR Ca^{2+} load and Ca^{2+} release, and its beat interval-dependent activity, may be reasonable candidate mechanisms underlying the beat interval dependency of alternans.

Indeed, using this approach, our model not only successfully reproduces the beat interval dependency of alternans, but it integrates alternans and various other I–F relations at the whole cell level via CaMKII involvement. Although it is intuitively clear that the role of CaMKII in Ca^{2+} handling and its time dependency are potentially important contributors to various I–F relations, no previous myocardial cell model has incorporated this, largely because of uncertainties in kinetic features. As a conceptual guide, however, the model has shown that it is not inconceivable for CaMKII to be an important contributor to alternans and it has advanced our integrative understanding of various I–F relations.

The mechanisms that underlie the various I–F relations consist of several components, including time-dependent recovery of RyR, SR Ca^{2+} load dependency of Ca^{2+} release, and probably time-dependent modification on Ca^{2+} release and uptake by CaMKII. These mechanisms are interdependent. In the model, CaMKII involvement in SR Ca^{2+} uptake is the causative mechanism of interval dependence of twitch duration, which enhances SR Ca^{2+} accumulation which, in turn, contributes to post-rest potentiation and the staircase phenomenon. SR Ca^{2+} load dependency of Ca^{2+} release is a key mechanism of alternans, and CaMKII involvement in SR Ca^{2+} load regulation enhances its beat interval dependency.

Another interesting point of the present study is that our model enables us to evaluate the effect of modulation of each Ca^{2+} handling pathway on alternans independently. This is useful when re-investigating possible mechanisms that may underlie the effects of various experimental interventions on alternans. For example, [Diaz *et al.* \(2002\)](#) reported that decreasing RyR open probability by applying tetracaine or via acidification produces alternans, and resulting Ca^{2+} transients are characterized by a slowing in rise and decay phases. Our investigation reproduced this behaviour, in principle, by slowing RyR dynamics, rather than decreasing their open probability.

Alternans is an integrated output of various Ca^{2+} handling components, each of which may affect it in different (partially counter-intuitive) ways. Even similar alternans patterns may be caused by different, even opposing, mechanisms. For example, our model can reproduce sustained alternans by any combination of alternans enhancing factors, such as increasing CaMKII involvement on RyR, slowing RyR and slowing Ca^{2+} uptake. It is quite difficult to experimentally control these factors separately and to identify the dominant factors. In that respect, the present model is useful for integrative studies into Ca^{2+} handling in alternans.

Limitations of this model are mainly related to its simplicity. The CaMKII kinetics model we use is conceptual, and not based on a detailed description of chemical reactions. [Dupont *et al.* \(2003\)](#) reported a more detailed biophysical model of CaMKII kinetics. However, we found that short-term responses of CaMKII activity to frequency changes in our model ([figure 2](#)) are consistent with the results obtained using the more complex models. Therefore, in terms of beat-by-beat short-term I–F relation, there is no significant difference between results with detailed and simple models.

Many of the recent more detailed Ca^{2+} dynamics models describe RyR as a cluster of unitary channels ([Greenstein & Winslow 2002](#); [Shiferaw *et al.* 2003](#)) to address spatially heterogenic effects within a cardiac cell (e.g. Ca^{2+} sparks or waves). [Diaz *et al.* \(2002\)](#) showed that subcellular alternans occurs randomly, so that the averaged whole cell signal would be quite uniform. Our point model does not address spatial heterogeneity, since we intended to make the model as simple as possible to clarify the effects of alterations in SR Ca^{2+} handling on I–F relation, especially on alternans. From the viewpoint of our aim, our phenomenological model offers a reasonable tool to describe underlying mechanisms.

Although altered SR Ca^{2+} handling is understood to be a primary mechanism underlying alternans, there is a possibility that the primary fluctuation of transmembrane Ca^{2+} fluxes plays an important role ([Fox *et al.* 2002](#); [Shiferaw *et al.* 2003](#)). The fact, however, that rapid pacing causes alternans, even under action potential clamp conditions, strongly suggests that SR Ca^{2+} handling is the dominant causative mechanism ([Chudin *et al.* 1999](#)). Still, the modelling study of alternans by [Shiferaw *et al.* \(2003\)](#) suggested that inactivation properties of the L-type Ca^{2+} channel may determine alternans, even during action potential clamp. Furthermore, it has been reported that I_{CaL} is affected by CaMKII ([Xiao *et al.* 1994](#); [Yuan & Bers 1994](#)), and that it shows beating interval-dependent behaviour ([Tseng 1988](#); [Hryshko & Bers 1990](#)). Therefore, the lack of CaMKII involvement in membrane currents is a limitation of the present model. Although the presented SR involvement is sufficient to explain a host of experimental observations involving I–F relations and alternans, further

investigations will benefit from incorporation into the model of a more detailed I_{CaL} model, with CaMKII and Ca^{2+} -dependent properties, such as proposed by Hund & Rudy (2004).

5. Conclusions

Thus, we present a cardiac cell model to simulate transient alternans during the decay of PESP, and its beat interval dependency. A key feature of this model is the involvement of CaMKII in Ca^{2+} handling. A conceptual CaMKII kinetics model that includes its slow inactivating properties was incorporated. The slow inactivation causes relatively increased CaMKII activity at shorter beat intervals. The SR load dependency of RyR Ca^{2+} release and SR Ca^{2+} uptake are modulated by CaMKII activity. Shorter beat intervals show alternans because of the steeper relation between SR load and release, due to the higher CaMKII activity that is a consequence of the shorter beat interval. The model suggests that CaMKII effects on Ca^{2+} handling are important not only for reproducing the beat interval dependency of alternans, but also for the integration of alternans and various other I–F relations at the whole cell level. Furthermore, the effects on alternans of various interventions, such as slowing or accelerating Ca^{2+} release and/or uptake, could be reproduced. We conclude that a slow time-dependent factor, represented in the model by CaMKII, is important for the integration of I–F relations, including alternans, and that our model offers a useful tool for analysing the roles of integrative Ca^{2+} handling in myocardial I–F relations.

Editors' note

Please see also related communications in this focussed issue by Leem *et al.* (2006) and Pásek *et al.* (2006).

The authors thank Dr Alan Garny and Dr Jeremy Rice for helpful comments on the manuscript. This study was supported by the British Heart Foundation. G.I. holds a PhD training grant from Eisai Co., Ltd.

Appendix A

All mathematical model equations and parameters (table 1) are listed in this section. Conceptual CaMKII kinetics is formulated in equation (A 49). CaMKII involvement on SR Ca^{2+} -dependent RyR recovery rate is formulated in equation (A 47). CaMKII involvement on SR Ca^{2+} uptake is formulated in equation (A 51). All membrane currents formulations are from Noble *et al.* (1991), except addition of voltage dependency on I_{NaK} . The force computation model is the one from Rice *et al.* (1999).

Membrane potential

$$\frac{dV}{dt} = \frac{-1}{C_m} (I_{Na} + I_{bNa} + I_{K1} + I_K + I_{to} + I_{bK} + I_{CaL} + I_{bCa} + I_{NaCa} + I_{NaK} + I_{Stim}). \quad (\text{A } 1)$$

Table 1. Model parameters.

R	gas constant	$8314 \text{ mJ K}^{-1} \text{ mol}^{-1}$
T	temperature	310 K
F	Faraday's constant	$96\,485 \text{ C mol}^{-1}$
C_m	membrane capacitance	$9.5 \times 10^{-5} \mu\text{F}$
v_i	myoplasmic volume	$1.6404 \times 10^{-5} \mu\text{l}$
v_{SR}	SR volume	$3.3477 \times 10^{-6} \mu\text{l}$
Na_o	extracellular Na^+ concentration	140.0 mM
K_o	extracellular K^+ concentration	4.0 mM
Ca_o	extracellular Ca^{2+} concentration	2.0 mM
G_{Na}	maximum I_{Na} conductance	$2.5 \mu\text{S}$
i_{Kmax}	maximum I_{K} current	1.0 nA
G_{K1}	maximum I_{K1} conductance	$1.0 \mu\text{S}$
$K_{m\text{K1}}$	K_o half-saturation constant of I_{K1}	10 mM
G_{to}	maximum I_{to} conductance	$0.005 \mu\text{S}$
P_{CaLCa}	maximum I_{CaL} conductance	0.25 nA mM^{-1}
$i_{\text{NaCa max}}$	maximum I_{NaCa} current	$5.0 \times 10^{-4} \text{ nA}$
γ	voltage dependence parameter of I_{NaCa}	0.5
$i_{\text{NaK max}}$	maximum I_{NaK}	1.36 nA
$K_{m\text{K}}$	K_o half-saturation constant of I_{NaK}	1 mM
$K_{m\text{Na}}$	Na_i half-saturation constant of I_{NaK}	21.7 mM
G_{bNa}	maximum I_{bNa} conductance	$6.0 \times 10^{-4} \mu\text{S}$
G_{bK}	maximum I_{bK} conductance	$6.0 \times 10^{-4} \mu\text{S}$
G_{bCa}	maximum I_{bCa} conductance	$2.5 \times 10^{-4} \mu\text{S}$
$K_{\text{rel max}}$	RyR release flux constant	500 s^{-1}
K_4	RyR transition rate from precursor to product fraction	1.8 s^{-1}
τ_{SRCaRyR}	time constant factor of effect of SR Ca^{2+} on RyR	0.05 s
τ_{CaMK}	time constant for CaMKII kinetics	0.8 s
V_{maxf}	SERCA forward rate parameter	0.292 mM s^{-1}
V_{maxr}	SERCA reverse rate parameter	0.391 mM s^{-1}
Cmdn_{tot}	total calmodulin concentration	0.02 mM
α_{cmdn}	Ca^{2+} on-rate for calmodulin	$10\,000 \text{ mM}^{-1} \text{ s}^{-1}$
β_{cmdn}	Ca^{2+} off-rate for calmodulin	500 s^{-1}
Trpn_{tot}	total troponin concentration	0.07 mM
α_{trpn}	Ca^{2+} on-rate for troponin	$80\,000 \text{ mM}^{-1} \text{ s}^{-1}$
β_{trpn}	maximum Ca^{2+} off-rate for troponin	200 s^{-1}
β_{tm}	reverse rate of tropomyosin shifting	40 s^{-1}
f_{XB}	basic transition rate from weak to strong crossbridge	10 s^{-1}
g_{XB}	minimum transition rate from strong to weak crossbridge	30 s^{-1}
SL	sarcomere length	$2.15 \mu\text{m}$
ζ	conversion factor for normalization to physiological force	0.1 N mm^{-2}
<i>initial conditions (2 Hz stimulation)</i>		
V	membrane potential	-94.015 mV
m	I_{Na} activation gate	1.3809×10^{-3}
h	I_{Na} inactivation gate	0.99569
x	I_{K} activation gate	5.1127×10^{-2}
r	I_{to} activation gate	1.5185×10^{-8}
s	I_{to} inactivation gate	0.95854
d	I_{Ca} activation gate	1.7908×10^{-8}
f	I_{Ca} inactivation gate	1.0

(Continued.)

Table 1. (Continued.)

F_{SRCaRyR}	effect factor of SR Ca^{2+} on RyR	0.25089
F_1	precursor fraction (RyR)	0.5268
F_2	activator fraction (RyR)	8.7508×10^{-6}
F_3	product fraction (RyR)	0.4732
F_{CaMK}	CaMKII activity factor	1.0280
Cmdn_{Ca}	concentration of Ca^{2+} bound to calmodulin	3.9636×10^{-6} mM
Trpn_{Ca}	concentration of Ca^{2+} bound to troponin	2.7661×10^{-4} mM
Na_i	intracellular Na^{2+} concentration	5.8041 mM
K_i	intracellular K^+ concentration	138.22 mM
Ca_i	myoplasmic Ca^{2+} concentration	9.91×10^{-6} mM
Ca_{SR}	SR Ca^{2+} concentration	0.24886 mM
N_0	non-permissive tropomyosin with 0 crossbridges	0.99917
P_0	permissive tropomyosin with 0 crossbridges	9.8593×10^{-5}
P_1	permissive tropomyosin with 1 crossbridge	1.3331×10^{-4}
P_2	permissive tropomyosin with 2 crossbridges	2.3505×10^{-4}
P_3	permissive tropomyosin with 3 crossbridges	1.5349×10^{-4}

Reversal potentials

$$E_{\text{Ca}} = \frac{RT}{2F} \ln \left(\frac{\text{Ca}_o}{\text{Ca}_i} \right), \quad (\text{A } 2)$$

$$E_{\text{Na}} = \frac{RT}{F} \ln \left(\frac{\text{Na}_o}{\text{Na}_i} \right), \quad (\text{A } 3)$$

$$E_{\text{K}} = \frac{RT}{F} \ln \left(\frac{K_o}{K_i} \right). \quad (\text{A } 4)$$

Fast Na^+ current (I_{Na})

$$I_{\text{Na}} = G_{\text{Na}} m^3 h (V - E_{mh}), \quad (\text{A } 5)$$

$$E_{mh} = \frac{RT}{F} \ln \left(\frac{\text{Na}_o + 0.12K_o}{\text{Na}_i + 0.12K_i} \right), \quad (\text{A } 6)$$

$$\frac{dm}{dt} = \alpha_m(1 - m) - \beta_m m, \quad (\text{A } 7)$$

$$\frac{dh}{dt} = \alpha_h(1 - h) - \beta_h h, \quad (\text{A } 8)$$

$$\alpha_m = \frac{200(V + 41)}{1 - e^{-0.1(V+41)}}, \quad (\text{A } 9)$$

$$\beta_m = 8000 e^{-0.056(V+66)}, \quad (\text{A } 10)$$

$$\alpha_h = 20 e^{-0.125(V+75)}, \quad (\text{A } 11)$$

$$\beta_h = \frac{2000}{1 + 320 e^{-0.1(V+75)}}. \quad (\text{A } 12)$$

Time-dependent rectifier K^+ current (I_K)

$$I_K = \frac{i_{K\max}x(K_i - K_o e^{-VF/RT})}{140}, \quad (\text{A } 13)$$

$$\frac{dx}{dt} = \alpha_x(1-x) - \beta_x x, \quad (\text{A } 14)$$

$$\alpha_x = \frac{0.5 e^{0.0826(V+50)}}{1 + e^{0.057(V+50)}}, \quad (\text{A } 15)$$

$$\beta_x = \frac{1.3 e^{-0.06(V+20)}}{1 + e^{-0.04(V+20)}}. \quad (\text{A } 16)$$

Time-independent rectifier K^+ current (I_{K1})

$$I_{K1} = \frac{G_{K1}(V - E_K) \frac{K_o}{K_o + K_{mK1}}}{1 + e^{2F(V - E_K - 10)/RT}}. \quad (\text{A } 17)$$

Transient outward K^+ current (I_{to})

$$I_{to} = G_{to}rs(V - EK), \quad (\text{A } 18)$$

$$\frac{dr}{dt} = 333 \left(\frac{1}{1 + e^{-0.2(V+4)}} - r \right), \quad (\text{A } 19)$$

$$\frac{ds}{dt} = \alpha_s(1-s) - \beta_s s, \quad (\text{A } 20)$$

$$\alpha_s = 0.033 e^{-V/17}, \quad (\text{A } 21)$$

$$\beta_s = \frac{33}{1 + e^{-0.125(V+10)}}. \quad (\text{A } 22)$$

L-type Ca^{2+} current (I_{CaL})

$$I_{CaL} = I_{CaLCa} + I_{CaLK} + I_{CaLNa}, \quad (\text{A } 23)$$

$$I_{CaLCa} = 4df \frac{P_{CaLCa}(V-50)F/RT}{1 - e^{-2(V-50)F/RT}} (Ca_i e^{100F/RT} - Ca_o e^{-2F(V-50)/RT}), \quad (\text{A } 24)$$

$$I_{CaLK} = 0.002df \frac{P_{CaLCa}(V-50)F/RT}{1 - e^{-(V-50)F/RT}} (K_i e^{50F/RT} - K_o e^{-F(V-50)/RT}), \quad (\text{A } 25)$$

$$I_{CaLNa} = 0.01df \frac{P_{CaLCa}(V-50)F/RT}{1 - e^{-(V-50)F/RT}} (Na_i e^{50F/RT} - Na_o e^{-F(V-50)/RT}), \quad (\text{A } 26)$$

$$\frac{dd}{dt} = \alpha_d(1-d) - \beta_d d, \quad (\text{A } 27)$$

$$\alpha_d = \frac{90(V + 19)}{1 - e^{-0.25(V+19)}}, \quad (\text{A } 28)$$

$$\beta_d = \frac{-36(V + 19)}{1 - e^{0.1(V+19)}}, \quad (\text{A } 29)$$

$$\frac{df}{dt} = \alpha_f(1 - f) - \beta_f f, \quad (\text{A } 30)$$

$$\alpha_f = \frac{3.125(V + 34)}{-1 + e^{0.25(V+34)}}, \quad (\text{A } 31)$$

$$\beta_f = \frac{25}{1 + e^{-0.25(V+34)}}. \quad (\text{A } 32)$$

Na⁺/Ca²⁺ exchanger current (I_{NaCa})

$$I_{\text{NaCa}} = i_{\text{NaCa max}} \frac{e^{\gamma VF/RT} \text{Na}_i^3 \text{Ca}_o - e^{(\gamma-1)VF/RT} \text{Na}_o^3 \text{Ca}_i}{1 + \frac{\text{Ca}_i}{0.0069}}. \quad (\text{A } 33)$$

Na⁺/K⁺ pump current (I_{NaK})

$$I_{\text{NaK}} = i_{\text{NaK max}} \left(\frac{K_o}{K_o + K_{mK}} \right) \left(\frac{\text{Na}_i}{\text{Na}_i + K_{m\text{Na}}} \right) \times \left(\frac{1}{1 + 0.1245 e^{-0.1VF/RT} + 0.0353 e^{-VF/RT}} \right). \quad (\text{A } 34)$$

Background currents

$$I_{\text{bCa}} = G_{\text{bCa}}(V - E_{\text{Ca}}), \quad (\text{A } 35)$$

$$I_{\text{bK}} = G_{\text{bK}}(V - E_{\text{K}}), \quad (\text{A } 36)$$

$$I_{\text{bNa}} = G_{\text{bNa}}(V - E_{\text{Na}}). \quad (\text{A } 37)$$

SR Ca²⁺ handling
RyR channel Ca²⁺ release flux (J_{rel})

$$J_{\text{rel}} = K_{\text{rel}} F_{\text{rel}} (\text{Ca}_{\text{SR}} - \text{Ca}_i), \quad (\text{A } 38)$$

$$K_{\text{rel}} = K_{\text{rel max}} \frac{F_{\text{SRCaRyR}}}{F_{\text{SRCaRyR}} + 0.2}, \quad (\text{A } 39)$$

$$\frac{dF_{\text{SRCaRyR}}}{dt} = \frac{\text{Ca}_{\text{SR}} - F_{\text{SRCaRyR}}}{\tau_{\text{SRCaRyR}}}, \quad (\text{A } 40)$$

$$F_{\text{rel}} = \left(\frac{F_2}{F_2 + 0.25} \right)^2, \quad (\text{A } 41)$$

$$\frac{dF_1}{dt} = k_3 F_3 - k_4 F_1 - k_1 F_1, \quad (\text{A } 42)$$

$$\frac{dF_2}{dt} = k_1 F_1 - k_2 F_2, \quad (\text{A } 43)$$

$$\frac{dF_3}{dt} = k_2 F_2 - k_3 F_3 + k_4 F_1, \quad (\text{A } 44)$$

$$k_1 = 30\,625\,000 \text{Ca}_i^2 - 245 I_{\text{CaL}}, \quad (\text{A } 45)$$

$$k_2 = \frac{450}{1 + 0.36/\text{Ca}_{\text{SR}}}, \quad (\text{A } 46)$$

$$k_3 = 1.885 \left(\frac{F_{\text{SRCaRyR}}}{0.22} \right)^{N_{\text{CaMK}}}, \quad (\text{A } 47)$$

$$N_{\text{CaMK}} = \left(\frac{F_{\text{CaMK}}}{0.7} \right)^2, \quad (\text{A } 48)$$

$$\frac{dF_{\text{CaMK}}}{dt} = \frac{F_{\text{CaMK}\infty} - F_{\text{CaMK}}}{\tau_{\text{CaMK}}}, \quad (\text{A } 49)$$

$$F_{\text{CaMK}\infty} = \frac{\text{Cmdn}_{\text{Ca}}}{0.00005}. \quad (\text{A } 50)$$

SERCA pump Ca^{2+} uptake flux (J_{up})

$$J_{\text{up}} = \frac{F_{\text{CaMK}} V_{\text{max}} f_b - V_{\text{max}} r_b}{1 + f_b + r_b}, \quad (\text{A } 51)$$

$$f_b = \left(\frac{\text{Ca}_i}{0.00024} \right)^2, \quad (\text{A } 52)$$

$$r_b = \left(\frac{\text{Ca}_{\text{SR}}}{1.64} \right)^2. \quad (\text{A } 53)$$

Ca^{2+} buffers

$$\frac{d\text{Cmdn}_{\text{Ca}}}{dt} = \alpha_{\text{cmdn}} (\text{Cmdn}_{\text{tot}} - \text{Cmdn}_{\text{Ca}}) \text{Ca}_i - \beta_{\text{cmdn}} \text{Cmdn}_{\text{Ca}}, \quad (\text{A } 54)$$

$$\frac{d\text{Trpn}_{\text{Ca}}}{dt} = \alpha_{\text{trpn}} (\text{Trpn}_{\text{tot}} - \text{Trpn}_{\text{Ca}}) \text{Ca}_i - \beta_{\text{trpn}} \left[\frac{1 + 2(1 - \text{Force}_{\text{norm}})}{3} \right] \text{Trpn}_{\text{Ca}}. \quad (\text{A } 55)$$

Ionic concentration

$$\frac{dN_{a_i}}{dt} = -\frac{I_{Na} + I_{bNa} + I_{CaLNa} + 3I_{NaCa} + 3I_{NaK}}{v_i F}, \quad (\text{A } 56)$$

$$\frac{dK_i}{dt} = -\frac{I_{K1} + I_K + I_{to} + I_{bK} + I_{CaLK} - 2I_{NaK}}{v_i F}, \quad (\text{A } 57)$$

$$\frac{dC_{a_i}}{dt} = -\frac{I_{CaLCa} + I_{bCa} - 2I_{NaCa}}{2v_i F} - J_{up} + J_{rel} \frac{v_{SR}}{v_i} - \frac{dC_{mdnCa}}{dt} - \frac{dTrpnCa}{dt}, \quad (\text{A } 58)$$

$$\frac{dC_{aSR}}{dt} = J_{up} \frac{v_i}{v_{SR}} - J_{rel}. \quad (\text{A } 59)$$

Tropomyosin/crossbridge

$$\frac{dN0}{dt} = \beta_{tm} P0 - \alpha_{tm} N0 + g_{01} N1, \quad (\text{A } 60)$$

$$\frac{dP0}{dt} = -(\beta_{tm} + f_{01}) P0 + \alpha_{tm} N0 + g_{01} P1, \quad (\text{A } 61)$$

$$\frac{dP1}{dt} = -(\beta_{tm} + f_{12} + g_{01}) P1 + \alpha_{tm} N1 + f_{01} P0 + g_{12} P2, \quad (\text{A } 62)$$

$$\frac{dP2}{dt} = -(f_{23} + g_{12}) P2 + f_{12} P1 + g_{23} P3, \quad (\text{A } 63)$$

$$\frac{dP3}{dt} = -g_{23} P3 + f_{23} P2, \quad (\text{A } 64)$$

$$N1 = 1 - (N0 + P0 + P1 + P2 + P3), \quad (\text{A } 65)$$

$$\alpha_{tm} = \beta_{tm} \left(\frac{TrpnCa/Trpn_{tot}}{K_{tm}} \right)^{N_{tm}}, \quad (\text{A } 66)$$

$$K_{tm} = \frac{1}{1 + \frac{\beta_{trpn}/\alpha_{trpn}}{0.0017 - 0.0009SL_{norm}}}, \quad (\text{A } 67)$$

$$N_{tm} = 3.5 + 2.5SL_{norm}, \quad (\text{A } 68)$$

$$SL_{norm} = (SL - 1.7)/0.7, \quad (\text{A } 69)$$

$$f_{01} = 3f_{XB}, \quad (\text{A } 70)$$

$$f_{12} = 10f_{XB}, \quad (\text{A } 71)$$

$$f_{23} = 7f_{XB}, \quad (\text{A } 72)$$

$$g_{01} = g_{XB}(2 - \text{SL}_{\text{norm}}), \quad (\text{A } 73)$$

$$g_{12} = 2g_{XB}(2 - \text{SL}_{\text{norm}}), \quad (\text{A } 74)$$

$$g_{23} = 3g_{XB}(2 - \text{SL}_{\text{norm}}). \quad (\text{A } 75)$$

Force computation

$$\text{Force} = \zeta \text{Force}_{\text{norm}}, \quad (\text{A } 76)$$

$$\text{Force}_{\text{norm}} = \frac{\phi_{\text{SL}}(P1 + N1 + 2P2 + 3P3)}{\text{Force}_{\text{max}}}, \quad (\text{A } 77)$$

if $1.7 \mu\text{m} \leq \text{SL} \leq 2.0 \mu\text{m}$

$$\phi_{\text{SL}} = (\text{SL} - 0.6)/1.4,$$

if $2.0 \mu\text{m} \leq \text{SL} \leq 2.2 \mu\text{m}$

$$\phi_{\text{SL}} = 1,$$

if $2.2 \mu\text{m} \leq \text{SL} \leq 2.3 \mu\text{m}$

$$\phi_{\text{SL}} = (3.6 - \text{SL})/1.4, \quad (\text{A } 78)$$

$$\text{Force}_{\text{max}} = P1_{\text{max}} + 2P2_{\text{max}} + 3P3_{\text{max}}, \quad (\text{A } 79)$$

$$P1_{\text{max}} = \frac{(f_{01})(2g_{XB})(3g_{XB})}{\Sigma\text{paths}}, \quad (\text{A } 80)$$

$$P2_{\text{max}} = \frac{(f_{01})(f_{12})(3g_{XB})}{\Sigma\text{paths}}, \quad (\text{A } 81)$$

$$P3_{\text{max}} = \frac{(f_{01})(f_{12})(f_{23})}{\Sigma\text{paths}}, \quad (\text{A } 82)$$

$$\Sigma\text{paths} = (g_{XB})(2g_{XB})(3g_{XB}) + (f_{01})(2g_{XB})(3g_{XB}) + (f_{01})(f_{12})(3g_{XB}) + (f_{01})(f_{12})(f_{23}). \quad (\text{A } 83)$$

References

- Adler, D., Wong, A. Y. & Mahler, Y. 1985 Model of mechanical alternans in the mammalian myocardium. *J. Theor. Biol.* **117**, 563–577.
- Bassani, R. A., Mattiazzi, A. & Bers, D. M. 1995 CaMKII is responsible for activity-dependent acceleration of relaxation in rat ventricular myocytes. *Am. J. Physiol.* **268**, H703–H712.
- Braun, A. P. & Schulman, H. 1995 The multifunctional calcium/calmodulin-dependent protein kinase: from form to function. *Annu. Rev. Physiol.* **57**, 417–445. (doi:10.1146/annurev.ph.57.030195.002221)

- Ching, L. L., Williams, A. J. & Sitsapesan, R. 2000 Evidence for Ca^{2+} activation and inactivation sites on the luminal side of the cardiac ryanodine receptor complex. *Circ. Res.* **87**, 201–206.
- Chudin, E., Goldhaber, J., Garfinkel, A., Weiss, J. & Kogan, B. 1999 Intracellular Ca^{2+} dynamics and the stability of ventricular tachycardia. *Biophys. J.* **77**, 2930–2941.
- Davis, B. A., Schwartz, A., Samaha, F. J. & Kranias, E. G. 1983 Regulation of cardiac sarcoplasmic reticulum calcium transport by calcium-calmodulin-dependent phosphorylation. *J. Biol. Chem.* **258**, 13 587–13 591.
- Diaz, M. E., Eisner, D. A. & O'Neill, S. C. 2002 Depressed ryanodine receptor activity increases variability and duration of the systolic Ca^{2+} transient in rat ventricular myocytes. *Circ. Res.* **91**, 585–593. (doi:10.1161/01.RES.0000035527.53514.C2)
- Diaz, M. E., O'Neill, S. C. & Eisner, D. A. 2004 Sarcoplasmic reticulum calcium content fluctuation is the key to cardiac alternans. *Circ. Res.* **94**, 650–656. (doi:10.1161/01.RES.0000119923.64774.72)
- Dupont, G., Houart, G. & De Koninck, P. 2003 Sensitivity of CaM kinase II to the frequency of Ca^{2+} oscillations: a simple model. *Cell Calcium* **34**, 485–497. (doi:10.1016/S0143-4160(03)00152-0)
- Fox, J. J., McHarg, J. L. & Gilmour Jr, R. F. 2002 Ionic mechanism of electrical alternans. *Am. J. Physiol. Heart Circ. Physiol.* **282**, H516–H530.
- Greenstein, J. L. & Winslow, R. L. 2002 An integrative model of the cardiac ventricular myocyte incorporating local control of Ca^{2+} release. *Biophys. J.* **83**, 2918–2945.
- Gyorke, I. & Gyorke, S. 1998 Regulation of the cardiac ryanodine receptor channel by luminal Ca^{2+} involves luminal Ca^{2+} sensing sites. *Biophys. J.* **75**, 2801–2810.
- Hilgemann, D. W. & Noble, D. 1987 Excitation–contraction coupling and extracellular calcium transients in rabbit atrium: reconstruction of basic cellular mechanisms. *Proc. R. Soc. B* **230**, 163–205.
- Hryshko, L. V. & Bers, D. M. 1990 Ca current facilitation during postrest recovery depends on Ca entry. *Am. J. Physiol.* **259**, H951–H961.
- Hund, T. J. & Rudy, Y. 2004 Rate dependence and regulation of action potential and calcium transient in a canine cardiac ventricular cell model. *Circulation* **110**, 3168–3174. (doi:10.1161/01.CIR.0000147231.69595.D3)
- Iribe, G. *et al.* 2004 Arterial and left ventricular pressures illude transient alternans of contractility during postextrasystolic potentiation. *Jpn. J. Physiol.* **54**, 373–383. (doi:10.2170/jjphysiol.54.373)
- Kameyama, M., Hirayama, Y., Saitoh, H., Maruyama, M., Atarashi, H. & Takano, T. 2003 Possible contribution of the sarcoplasmic reticulum Ca^{2+} pump function to electrical and mechanical alternans. *J. Electrocardiol.* **36**, 125–135. (doi:10.1054/jelc.2003.50021)
- Kihara, Y. & Morgan, J. P. 1991 Abnormal Ca^{2+} handling is the primary cause of mechanical alternans: study in ferret ventricular muscles. *Am. J. Physiol.* **261**, H1746–H1755.
- Kockskamper, J., Zima, A. V. & Blatter, L. A. 2005 Modulation of sarcoplasmic reticulum Ca^{2+} release by glycolysis in cat atrial myocytes. *J. Physiol.* **564**, 697–714. (doi:10.1113/jphysiol.2004.078782)
- Kurihara, S. & Sakai, T. 1985 Effects of rapid cooling on mechanical and electrical responses in ventricular muscle of guinea-pig. *J. Physiol.* **361**, 361–378.
- Lab, M. J. & Seed, W. A. 1993 Pulsus alternans. *Cardiovasc. Res.* **27**, 1407–1412.
- Laurita, K. R., Katra, R., Wible, B., Wan, X. & Koo, M. H. 2003 Transmural heterogeneity of calcium handling in canine. *Circ. Res.* **92**, 668–675. (doi:10.1161/01.RES.0000062468.25308.27)
- Leem, C. H., Kim, W. T., Ha, J. M., Lee, Y. J., Seong, H. C., Choe, H., Jang, Y. J., Youm, J. B. & Earm, Y. E. 2006 Simulation of Ca^{2+} -activated Cl^- current of cardiomyocytes in rabbit pulmonary vein: implications of subsarcolemmal Ca^{2+} dynamics. *Phil. Trans. R. Soc. A* **364**, 1223–1243. (doi:10.1098/rsta.2006.1766)
- Li, L., Satoh, H., Ginsburg, K. S. & Bers, D. M. 1997 The effect of Ca^{2+} -calmodulin-dependent protein kinase II on cardiac excitation–contraction coupling in ferret ventricular myocytes. *J. Physiol.* **501**, 17–31. (doi:10.1111/j.1469-7793.1997.017bo.x)
- Maier, L. S. & Bers, D. M. 2002 Calcium, calmodulin, and calcium-calmodulin kinase II: heartbeat to heartbeat and beyond. *J. Mol. Cell. Cardiol.* **34**, 919–939. (doi:10.1006/jmcc.2002.2038)

- Maier, L. S., Bers, D. M. & Pieske, B. 2000 Differences in Ca²⁺-handling and sarcoplasmic reticulum Ca²⁺-content in isolated rat and rabbit myocardium. *J. Mol. Cell. Cardiol.* **32**, 2249–2258. (doi:10.1006/jmcc.2000.1252)
- Matsuoka, S., Sarai, N., Kuratomi, S., Ono, K. & Noma, A. 2003 Role of individual ionic current systems in ventricular cells hypothesized by a model study. *Jpn. J. Physiol.* **53**, 105–123. (doi:10.2170/jjphysiol.53.105)
- Meyer, T., Hanson, P. I., Stryer, L. & Schulman, H. 1992 Calmodulin trapping by calcium-calmodulin-dependent protein kinase. *Science* **256**, 1199–1202.
- Noble, D., Noble, S. J., Bett, G. C., Earm, Y. E., Ho, W. K. & So, I. K. 1991 The role of sodium-calcium exchange during the cardiac action potential. *Ann. N. Y. Acad. Sci.* **639**, 334–353.
- Noble, D., Varghese, A., Kohl, P. & Noble, P. 1998 Improved guinea-pig ventricular cell model incorporating a diadic space, IKr and IKs, and length- and tension-dependent processes. *Can. J. Cardiol.* **14**, 123–134.
- Nordin, C. 1993 Computer model of membrane current and intracellular Ca²⁺ flux in the isolated guinea pig ventricular myocyte. *Am. J. Physiol.* **265**, H2117–H2136.
- Pásek, M., Šimurda, J. & Christé, G. 2006 The functional role of cardiac T-tubules explored in a model of rat ventricular myocytes. *Phil. Trans. R. Soc. A* **364**, 1187–1206. (doi:10.1098/rsta.2006.1764)
- Pruvot, E. J., Katra, R. P., Rosenbaum, D. S. & Laurita, K. R. 2004 Role of calcium cycling versus restitution in the mechanism of repolarization alternans. *Circ. Res.* **94**, 1083–1090. (doi:10.1161/01.RES.0000125629.72053.95)
- Rice, J. J., Winslow, R. L. & Hunter, W. C. 1999 Comparison of putative cooperative mechanisms in cardiac muscle: length dependence and dynamic responses. *Am. J. Physiol.* **276**, H1734–H1754.
- Rice, J. J., Jafri, M. S. & Winslow, R. L. 2000 Modeling short-term interval–force relations in cardiac muscle. *Am. J. Physiol. Heart Circ. Physiol.* **278**, H913–H931.
- Schouten, V. J. 1990 Interval dependence of force and twitch duration in rat heart explained by Ca²⁺ pump inactivation in sarcoplasmic reticulum. *J. Physiol. (Lond.)* **431**, 427–444.
- Shannon, T. R., Ginsburg, K. S. & Bers, D. M. 2000 Reverse mode of the sarcoplasmic reticulum calcium pump and load-dependent cytosolic calcium decline in voltage-clamped cardiac ventricular myocytes. *Biophys. J.* **78**, 322–333.
- Shannon, T. R., Guo, T. & Bers, D. M. 2003 Ca²⁺ scraps: local depletions of free [Ca²⁺] in cardiac sarcoplasmic reticulum during contractions leave substantial Ca²⁺ reserve. *Circ. Res.* **93**, 40–45. (doi:10.1161/01.RES.0000079967.11815.19)
- Shiferaw, Y., Watanabe, M. A., Garfinkel, A., Weiss, J. N. & Karma, A. 2003 Model of intracellular calcium cycling in ventricular myocytes. *Biophys. J.* **85**, 3666–3686.
- Shimizu, J. *et al.* 2000 Postextrasystolic contractile decay always contains exponential and alternans components in canine heart. *Am. J. Physiol. Heart Circ. Physiol.* **279**, H225–H233.
- Snyder, S. M., Palmer, B. M. & Moore, R. L. 2000 A mathematical model of cardiocyte Ca²⁺ dynamics with a novel representation of sarcoplasmic reticular Ca²⁺ control. *Biophys. J.* **79**, 94–115.
- Tameyasu, T. 2002 Model for the regulation of Ca²⁺ release from the sarcoplasmic reticulum in heart muscle. *Jpn. J. Physiol.* **52**, 57–68. (doi:10.2170/jjphysiol.52.57)
- Tseng, G. N. 1988 Calcium current restitution in mammalian ventricular myocytes is modulated by intracellular calcium. *Circ. Res.* **63**, 468–482.
- Wier, W. G. & Yue, D. T. 1986 Intracellular calcium transients underlying the short-term force–interval relationship in ferret ventricular myocardium. *J. Physiol. (Lond.)* **376**, 507–530.
- Witcher, D. R., Kovacs, R. J., Schulman, H., Cefali, D. C. & Jones, L. R. 1991 Unique phosphorylation site on the cardiac ryanodine receptor regulates calcium channel activity. *J. Biol. Chem.* **266**, 11 144–11 152.
- Xiao, R. P., Cheng, H., Lederer, W. J., Suzuki, T. & Lakatta, E. G. 1994 Dual regulation of Ca²⁺/calmodulin-dependent kinase II activity by membrane voltage and by calcium influx. *Proc. Natl Acad. Sci. USA* **91**, 9659–9663.
- Yuan, W. & Bers, D. M. 1994 Ca-dependent facilitation of cardiac Ca current is due to Ca-calmodulin-dependent protein kinase. *Am. J. Physiol.* **267**, H982–H993.